Frontiers in Bioscience Landmark

Front. Biosci. (Landmark Ed) **2026**; 31(11): 55797
https://doi.org/10.31083/FBL55797

Original Research

GPRC5A Contributes to Colorectal Cancer Liver Metastasis Through a THBS1/PI3K/AKT-Associated Mechanism

Lei Hu[1,2], Zihao Du[1], Xinyu Jiang[1], Mengjuan Li[1], Weiwei Li[1], Wenkang Yuan[1], Canliang Lu[1], Chao Zhang[1,*], Chong Zhang[1,*]

[1]Department of General Surgery, The First Affiliated Hospital of Anhui Medical University, 230022 Hefei, Anhui, China
[2]Department of General Surgery, Tongling People's Hospital, 244000 Tongling, Anhui, China
*Correspondence: chaozhang@fy.ahmu.edu.cn (Chao Zhang); zhangchong@fy.ahmu.edu.cn (Chong Zhang)
Academic Editor: Amancio Carnero Moya
Submitted: 9 July 2026 Revised: 20 September 2026 Accepted: 9 October 2026 Published: 18 November 2026

Abstract

Background: Liver metastasis is the leading cause of death in patients with colorectal cancer (CRC). The molecular mechanisms underlying colorectal liver metastasis (CRLM) remain incompletely understood. Although G protein-coupled receptor class C group 5 member A (GPRC5A) has been implicated in tumor progression, its role in CRLM remains unknown. **Methods:** We conducted integrative analyses of public bulk transcriptomic datasets to evaluate GPRC5A expression in response to retinoic acid and its clinical relevance in CRLM. *In vitro* and *in vivo* functional assays were conducted using GPRC5A-knockdown and thrombospondin 1 (THBS1)-overexpressing cell lines. The effects of pharmacological interference with THBS1-mediated signaling were evaluated using LSKL in a mouse model to assess its potential therapeutic relevance. **Results:** GPRC5A was markedly upregulated in liver metastatic lesions, and elevated expression correlated with worse progression-free survival and overall survival. GPRC5A knockdown significantly inhibited the proliferation, migration, and hepatic metastatic capacity of CRC cells in both cell culture and animal models. Mechanistically, GPRC5A depletion downregulated THBS1 expression and partially reduced phosphoinositide 3-kinase/protein kinase B (PI3K/AKT) phosphorylation without affecting total PI3K and AKT protein levels. Importantly, forced THBS1 overexpression partially rescued the malignant phenotypes and restored PI3K/AKT activation in GPRC5A-deficient cells. *In vivo*, administration of LSKL, a THBS1-derived inhibitory peptide that interferes with THBS1-mediated activation of latent TGF-β, substantially reduced the liver metastatic burden. **Conclusions:** This study suggests a potential GPRC5A-THBS1-PI3K/AKT signaling axis associated with CRLM progression. Our findings provide a mechanistic basis for further investigating this pathway and offer a preclinical rationale for targeting THBS1 as a potential therapeutic strategy against CRLM.

Keywords: cancer; colorectal cancer liver metastasis (CRLM)

1. Introduction

Colorectal cancer (CRC) is the third most frequent cancer type worldwide and the second most common cause of cancer-related death [1,2]. About 50% of patients with CRC ultimately develop colorectal liver metastasis (CRLM), with subsequent liver failure being the primary cause of mortality [3,4]. Comprehensive treatment modalities include surgical resection, targeted therapy, and immunotherapy. Despite the continuous advances in treatment, 5-year survival rates for CRLM patients remain low, with therapeutic resistance and recurrence posing significant challenges [5,6]. Hence, there is a pressing clinical need to better understand the molecular mechanisms underlying CRLM and to identify novel therapeutic targets.

G protein-coupled receptor class C group 5 member A (GPRC5A) is a retinoic acid-inducible member of the GPCR superfamily that was initially characterized as a mediator of retinoid signaling during cell differentiation [7]. Recent findings indicate that GPRC5A is a critical and context-dependent regulator of tumor initiation and progression [8,9]. In pancreatic cancer [10], breast cancer [11], and glioblastoma [12], GPRC5A frequently functions as an oncogene, with its overexpression strongly associated with poor prognosis. In CRC, recent single-cell transcriptomic and multi-omics integrative analyses have suggested that GPRC5A may be a candidate driver of malignant progression and metastasis [13,14]. Nevertheless, the GPRC5A expression profile, biological functions, and key molecular mechanisms in liver metastasis remain unknown.

Through integrative analysis of public transcriptomic datasets, we found that GPRC5A was upregulated in CRLM and correlated with poor survival. Functional assays, both *in vitro* and *in vivo*, revealed that GPRC5A promotes CRC cell proliferation, migration, and hepatic metastasis. Mechanistically, GPRC5A upregulates thrombospondin 1 (THBS1), which then activates phosphorylation of phosphoinositide 3-kinase/protein kinase B (PI3K/AKT). Importantly, restoration of THBS1 effectively rescues the malignant phenotypes suppressed by GPRC5A knockdown. Furthermore, pharmacological inhibition of THBS1 in a mouse model of liver metastasis was shown to validate the therapeutic potential of targeting this pathway. Overall, our

Copyright: © 2026 The Author(s). Published by IMR Press.
This is an open access article under the CC BY 4.0 license.

Publisher's Note: IMR Press stays neutral with regard to jurisdictional claims in published maps and institutional affiliations.

results suggest a potential GPRC5A-THBS1-PI3K/AKT signaling axis associated with CRLM progression, providing a rationale for further exploration of this pathway as a potential therapeutic target.

2. Materials and Methods

2.1 Tissue Samples and Patients

Matching CRLM and adjacent normal liver tissues from CRC patients who underwent radical surgery at the First Affiliated Hospital of Anhui Medical University were collected and stored. All nine patients provided paired CRLM and adjacent normal liver tissue samples, and all tissue samples were obtained from the same patient cohort. No preoperative chemotherapy, radiotherapy, immunotherapy, or targeted therapy had been given to any of these patients. The Ethics Committee of the First Affiliated Hospital of Anhui Medical University approved this research, which adhered to the principles of the Declaration of Helsinki. All participants provided written informed consent (**Supplementary Table 1**).

2.2 Extraction and Processing of Public Transcriptomic Data

The National Center for Biotechnology Information was used to extract publicly available transcriptomic datasets from The Cancer Genome Atlas (TCGA) and Gene Expression Omnibus (GEO). Gene expression profiles from the GSE41258 and TCGA pan-cancer cohorts were included. Clinical and survival data from TCGA-COAD and TCGA-READ cohorts were collected for prognostic analyses. All data processing and analyses were conducted with the Home for Researchers platform (https://www.home-for-researchers.com/) following standardized bioinformatics workflows.

2.3 Cell Culture

The CT26 mouse colorectal cancer cell line was purchased from the American Type Culture Collection (ATCC, CRL-2638; Manassas, VA, USA) and authenticated by STR profiling. It tested negative for mycoplasma contamination. The cells were grown at 37 °C in RPMI-1640 medium containing 10% fetal bovine serum (FBS) and 1% penicillin-streptomycin in a humidified atmosphere containing 5% CO_2.

2.4 Quantitative Real-Time PCR (qRT-PCR)

TRIzol Reagent (Cat. No. 15596-018, Invitrogen, Carlsbad, CA, USA) was used to extract total RNA from tissues and cells as recommended by the manufacturer. PrimeScript RT Master Mix (Perfect Real Time) (Cat. No. RR036, Takara Bio Inc., Kusatsu, Shiga, Japan) was used to synthesize complementary DNA (cDNA). qRT-PCR was conducted using TB Green Premix Ex Taq II (Tli RNaseH Plus) (Cat. No. RR820, Takara Bio Inc., Kusatsu, Shiga, Japan) with a LightCycler 480 System (Roche Diagnostics International Ltd., Rotkreuz, Switzerland) and using primer sequences shown in **Supplementary Table 2**.

2.5 Western Blotting

Lysis buffer containing protease and phosphatase inhibitors was used to extract total protein from tissues and cells. Samples containing equal amounts of protein were resolved on SDS-PAGE gel electrophoresis and subsequently blotted onto nitrocellulose membranes. These were blocked with 5% non-fat milk, incubated overnight at 4 °C with primary antibodies, then incubated for 1.5 h at room temperature with corresponding secondary antibodies. An enhanced chemiluminescence kit was used to visualize the protein bands, followed by quantification with ImageJ (version 1.53; National Institutes of Health, Bethesda, MD, USA). **Supplementary Table 3** provides details of the antibodies used.

2.6 Immunohistochemistry (IHC)

After fixation and dehydration, patient tumor tissues and mouse liver samples were embedded in paraffin and cut into 4 µm-thick sections. These were subsequently deparaffinized, rehydrated, and microwaved for 30 min in citrate buffer (pH 6.0) for antigen retrieval. The activity of endogenous peroxidase was blocked by 15-min incubation with 3% H_2O_2. Sections were then blocked with 5% bovine serum albumin (30 min, room temperature) before incubation with primary antibody (4 °C, overnight), followed by secondary antibody (1 h, room temperature). The chromogen used was DAB, with hematoxylin applied for counterstaining. Images were recorded with an upright microscope, and Image-Pro Plus (version 6.0; Media Cybernetics, Rockville, MD, USA) was employed to quantify immunohistochemical staining. For each tissue section, five randomly selected and representative high-power fields were captured under identical microscope settings. The integrated optical density (IOD) and corresponding positive staining area were evaluated. Mean optical density (MOD), calculated as IOD/area, was used to determine the expression of target proteins. To minimize observer bias, the image acquisition and quantitative analyses were conducted under blinded conditions.

2.7 shRNA Construction and Lentiviral Transduction

Short hairpin RNAs (shRNAs) that target murine GPRC5A (shGPRC5A#1/2/3), as well as the negative control (shNC), were synthesized and cloned into lentiviral vectors. CT26 cells were grown in 6-well plates to around 50% confluence. Lentiviral particles were then added to the adherent cells and incubated for 48 h. Cells with stable knockdown were selected by culturing in fresh RPMI-1640 medium with 5 µg/mL puromycin. **Supplementary Table 4** lists the shRNA target sequences.

2.8 Cell Proliferation Assay (Cell Counting Kit-8, CCK-8)

Stably transduced CT26 cells were seeded into 96-well plates (5×10^3 cells per well) and grown for 24, 48, and 72 h. After adding CCK-8 solution (Cat. No. G4103, Wuhan Servicebio Technology Co., Ltd., Wuhan, Hubei, China) to each well, absorbance at 450 nm was measured with a microplate reader.

2.9 Wound Healing Assay

Cells were grown in 6-well plates until they reached approximately 95% confluence. Each well was scratched in a straight line with a 200 µL sterile tip, washed three times with PBS, and then supplemented with fresh RPMI-1640 medium containing 2% FBS. The scratched area was photographed at 0 and 48 h with a microscope, and wound closure was then evaluated with ImageJ software.

2.10 Transwell Migration Assay

Serum-free RPMI-1640 medium (200 µL) containing 5×10^5 cells was added to the upper chamber of Transwell inserts (8 µm pore size). The lower chamber contained 600 µL RPMI-1640 medium with 10% FBS. After 24 h incubation (37 °C, 5% CO_2), cells on the lower membrane surface were methanol-fixed and stained with 0.1% crystal violet. The number of migrated cells was subsequently evaluated using photographs taken with an upright microscope and ImageJ software.

2.11 RNA Sequencing and Bioinformatics Analysis

Total RNA was extracted using TRIzol reagent (Magen, Guangzhou, Guangdong, China). Three biological replicates were included per group. RNA quality was assessed using a NanoDrop ND-2000 spectrophotometer (Thermo Fisher Scientific, Wilmington, DE, USA) and an Agilent 4150 Bioanalyzer (Agilent Technologies, Santa Clara, CA, USA). Only samples with OD260/280 ratios of 1.8–2.1, OD260/230 ratios >2.0, and RNA integrity number (RIN) ≥7.0 were used for library preparation. Libraries were prepared using the ABclonal mRNA-seq Library Preparation Kit (ABclonal, Wuhan, Hubei, China) and sequenced on the Illumina NovaSeq X Plus platform (Illumina, San Diego, CA, USA). Raw reads were filtered using fastp (v0.23.2, OpenGene) and aligned to the Mus musculus reference genome (GRCm39) using HISAT2 (v2.2.1, Daehwan Kim Laboratory). Gene counts were generated with FeatureCounts (v2.0.3, Subread), and expression levels were normalized as Fragments Per Kilobase of transcript per Million mapped reads (FPKM). Differential expression analysis was performed using DESeq2 (v1.40.2, Bioconductor). Genes with $|\log2 \text{ fold change}| > 1$ and adjusted p-value < 0.05 were considered differentially expressed. Gene Ontology (GO) and Kyoto Encyclopedia of Genes and Genomes (KEGG) enrichment analyses were conducted using clusterProfiler (v4.8.3, Bioconductor), with adjusted p-value < 0.05 considered statistically significant.

2.12 Induction of the Animal Model and Treatment

All animal experiments were performed using 5–8-week-old male BALB/c mice obtained from GemPharmatech Co., Ltd. (Jiangsu, China). The mice were specific pathogen-free (SPF) and immunocompetent, with a normal immune status. All mice were genetically unmodified wild-type BALB/c mice. No previous experimental treatments were administered before the initiation of the study. Each experimental group consisted of six mice (n = 6 per group). Different figures represent independent experimental cohorts conducted separately. Mice were anesthetized with isoflurane inhalation before the procedure. For the induction of liver metastasis, luciferase-labeled tumor cells (1×10^6) were resuspended in 100 µL of PBS and injected into the spleen. Tumor progression was monitored dynamically by bioluminescence imaging performed once per week for 4 weeks. Briefly, mice under anesthesia received an intraperitoneal injection of D-luciferin (Beyotime, China) at a dose of 150 mg/kg body weight, and a Tanon imaging system (Tanon Science & Technology Co., Ltd., Shanghai, China) was subsequently used to detect the luminescent signals. Following confirmation of hepatic metastases, mice were randomly assigned to the treatment groups, comprising IgG isotype control antibody (intraperitoneal injection, 2 µg per dose, once every other day) and LSKL (intraperitoneal injection, 4 mg/kg/day) [15]. After 4 weeks of treatment, all mice were sacrificed and the tissues collected for experimental analysis. Mice were deeply anesthetized with 2.0%–2.5% isoflurane and subsequently euthanized by cervical dislocation. Histological evaluation and quantification of liver metastatic burden were performed in a blinded manner. Animal experiments were conducted in accordance with animal welfare regulations and were approved by the Animal Ethics Committee, Anhui Medical University. To minimize potential observer bias, histological assessment of the liver metastatic burden was conducted by investigators who were blinded to allocation of the experimental group. No animals were excluded from the analysis in any experimental group.

2.13 Statistical Analyses

Data are presented as mean ± standard deviation, with data distribution illustrated by individual data points. Two groups were compared by two-tailed unpaired Student's t-test or the Wilcoxon rank-sum test, while one- or two-way analysis of variance was performed to compare multiple groups. Kaplan-Meier analysis was used to evaluate overall survival (OS) and progression-free survival (PFS), with the log-rank test used to assess differences between groups. Statistical analyses were performed using GraphPad Prism (version 9.0; GraphPad Software, San Diego, CA, USA). A p-value < 0.05 was considered statistically significant. Statistical significance was indicated as: ns, non-significant; *p < 0.05; **p < 0.01; ***p < 0.001; ****p < 0.0001.

3. Results

3.1 Elevated GPRC5A Expression in CRLM and Correlation With Poor Prognosis

We first performed an integrated analysis of the GSE41258 dataset of CRLM to identify potential targets. The GPRC5A expression was found to be significantly elevated in tumor (Fig. 1A,B). High GPRC5A expression was observed in liver metastases from the GSE41258 dataset (Fig. 1C). In line with this, higher GPRC5A mRNA and protein levels were found in liver metastatic tumor tissue than in adjacent normal tissue (Fig. 1D,E). This upregulation of GPRC5A was further confirmed by IHC (Fig. 1F). Pan-cancer expression analysis showed that GPRC5A is markedly overexpressed in a number of gastrointestinal malignancies, including gastric cancer and CRC, compared with corresponding normal tissues (Fig. 1G). Moreover, elevated GPRC5A expression was associated with significantly shorter OS and PFS in CRC patients (Fig. 1H). Together, the results suggest that elevated GPRC5A expression correlates with poor outcomes in CRC patients.

3.2 GPRC5A Promotes Development of Liver Metastasis

We next investigated the role of GPRC5A in tumor progression by establishing GPRC5A-knockdown CT26 cells (shGPRC5A) and corresponding empty vector control cells (shNC). Knockdown efficiency was verified at both the mRNA and protein levels (Fig. 2A,B). GPRC5A knockdown significantly suppressed tumor cell proliferation (Fig. 2C). Moreover, the migratory capacity of tumor cells was markedly attenuated upon depletion of GPRC5A (Fig. 2D,E). The *in vivo* effect of GPRC5A on CRLM was examined by establishing a mouse model of liver metastasis via intrasplenic injection. Compared to mice injected with shNC cells, those receiving shGPRC5A cells exhibited a dramatic reduction in hepatic luminescence signal intensity, along with decreased liver weight and a lower metastatic burden in the liver (Fig. 2F–J).

3.3 GPRC5A Is Associated With THBS1 Expression and PI3K/AKT Phosphorylation

RNA-seq was performed in GPRC5A-knockdown tumor cells to investigate how GPRC5A mediates tumor progression. This analysis identified THBS1 as a strongly downregulated gene following GPRC5A depletion, with the lowest adjusted *p*-value among the differentially expressed genes (**Supplementary Table 5**). Further analysis of mRNA and protein levels confirmed this finding (Fig. 3A–C). KEGG enrichment analysis revealed that GPRC5A was significantly associated with enrichment of the PI3K/AKT pathway (Fig. 3D). A significant positive correlation was observed between THBS1 expression and the PI3K/AKT pathway (Fig. 3E). We therefore overexpressed THBS1 in the GPRC5A-knockdown cell line and confirmed changes at both mRNA and protein levels (Fig. 3F,G). Neither GPRC5A nor THBS1 alterations were found to affect total PI3K or AKT protein levels. However, GPRC5A knockdown markedly suppressed phosphorylation of PI3K/AKT, which was rescued by subsequent THBS1 overexpression (Fig. 3H). Collectively, these results suggest that GPRC5A may influence PI3K/AKT phosphorylation in association with THBS1.

3.4 GPRC5A Promotes Tumor Progression in Association With THBS1/PI3K/AKT Signaling

To determine whether THBS1 is a key downstream effector mediating the tumor-promoting function of GPRC5A, THBS1 was first overexpressed in GPRC5A-knockdown CT26 cells, and several rescue experiments were subsequently conducted. Results from CCK-8 assays demonstrated that THBS1 overexpression partially reversed the reduction in cell proliferation caused by GPRC5A knockdown (Fig. 4A). In addition, transwell and wound-healing assays revealed that THBS1 overexpression partially repaired the defects in migration caused by GPRC5A depletion (Fig. 4B,C). We next established the murine liver metastasis model and performed dynamic monitoring via *in vivo* imaging. In line with the *in vitro* findings, THBS1 overexpression partially restored the hepatic colonization and growth of GPRC5A-knockdown cells, as evidenced by the recovery of luminescence signal intensity and increased liver weight and metastatic burden (Fig. 4D–H). Moreover, Western blot analysis of liver metastatic tissues confirmed that GPRC5A knockdown suppressed phosphorylation of the PI3K/AKT pathway, whereas THBS1 overexpression partially restored p-AKT levels *in vivo*, in agreement with the *in vitro* mechanistic observations (Fig. 4I). Collectively, these functional experiments support a role for GPRC5A in CRC cell proliferation, migration, and liver metastatic progression, potentially in association with THBS1 and PI3K/AKT signaling.

3.5 Targeting THBS1 Inhibits the Progression of CRLM

To validate the therapeutic relevance of THBS1, mice bearing liver metastases were treated with LSKL, a pharmacological tool to block THBS1-mediated signaling. The results of *in vivo* imaging revealed that the LSKL-treated group had significantly decreased liver metastatic burden compared with the control group (Fig. 5A,B). No significant change was seen in body weight, whereas liver weight and the extent of liver metastases were both significantly lower (Fig. 5C–F). These results indicate that targeting THBS1 can effectively suppress the progression of CRC liver metastasis.

4. Discussion

The molecular mechanisms driving CRLM remain incompletely understood, and there is a pressing need to find novel drivers and actionable targets. This study revealed for the first time the pro-metastatic function of GPRC5A in CRLM. Furthermore, it identified THBS1 as a critical

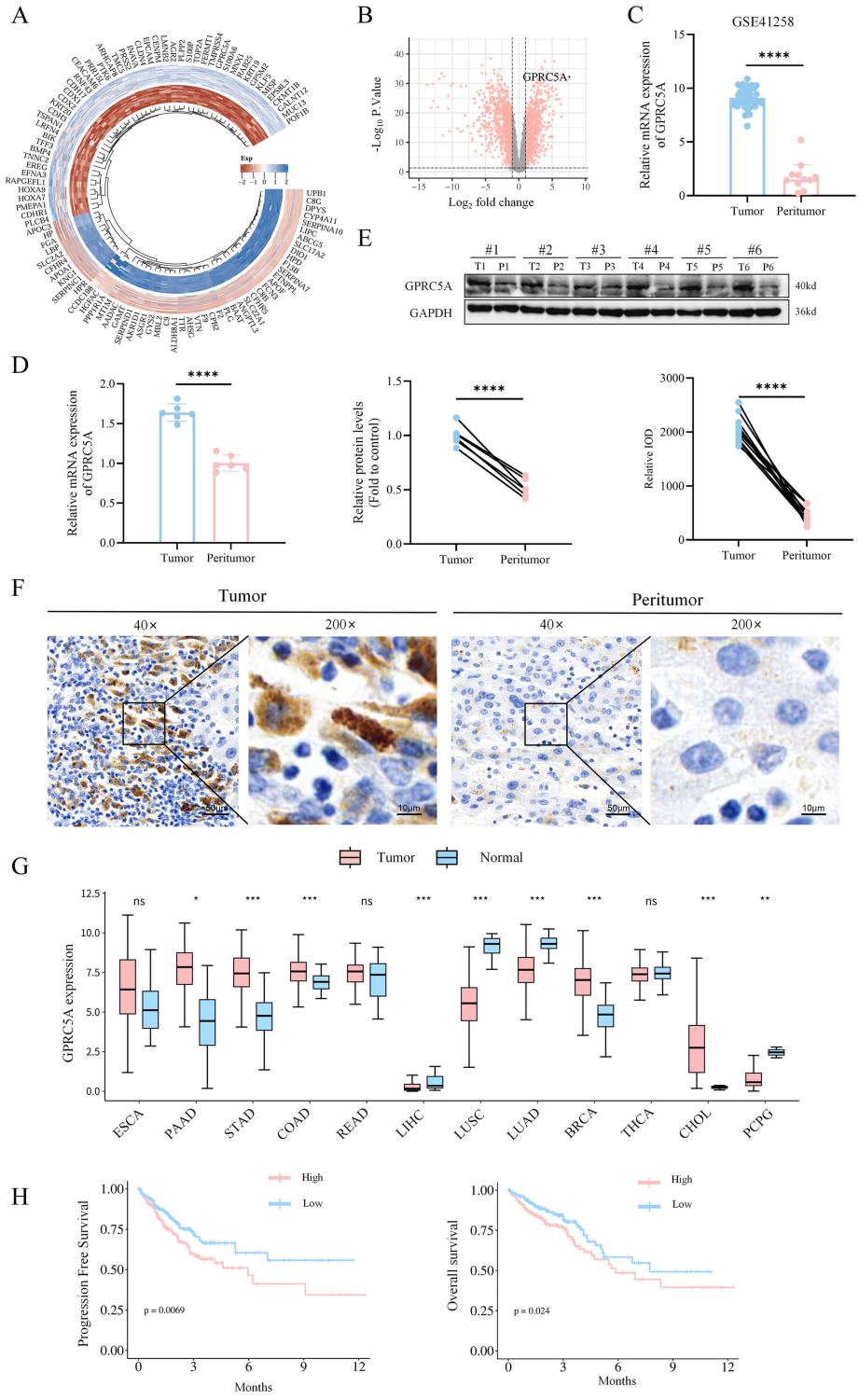


Fig. 1. Elevated G protein-coupled receptor class C group 5 member A (GPRC5A) expression in colorectal liver metastasis (CRLM) is associated with worse survival. (A,B) Heatmap (A) and volcano plot (B) analyses of the GSE41258 dataset showing significant upregulation of GPRC5A in tumor tissues. (C) GPRC5A expression in the GSE41258 dataset. (D,E) GPRC5A mRNA and protein levels in CRLM and adjacent peritumor samples (n = 6). (F) Immunostaining of GPRC5A in tumor and adjacent normal tissues from a representative human CRLM case (n = 9). 40× magnification: scale bar = 50 μm; 200× magnification: scale bar = 10 μm. (G) Differential GPRC5A expression across different tumor types in The Cancer Genome Atlas (TCGA) compared with normal tissues. (H) Kaplan-Meier survival analysis of Colon adenocarcinoma (COAD) and rectum adenocarcinoma (READ) patients from TCGA with low or high GPRC5A levels. ns > 0.05, *p < 0.05, **p < 0.01, ***p < 0.001, ****p < 0.0001.

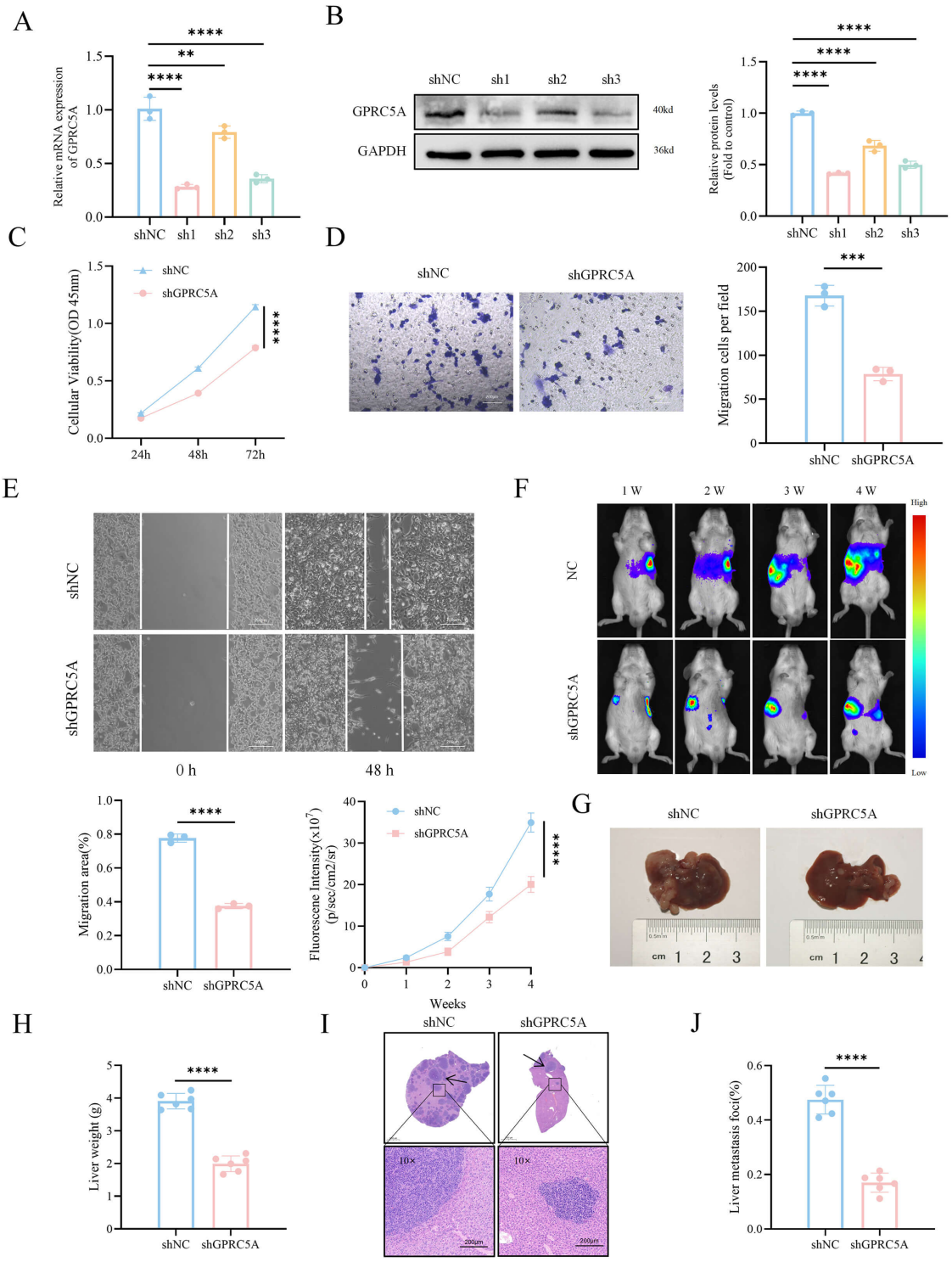


Fig. 2. GPRC5A promotes the development and progression of liver metastasis. (A,B) The GPRC5A knockdown efficiency in CT26 cells was demonstrated at the mRNA and protein levels (n = 3). (C) The CCK-8 assay was performed to determine cell viability (n = 6). (D) Representative images and the corresponding number of cells from transwell assays with shNC and shGPRC5A cell lines. 10× magnification: scale bar = 200 μm. (E) Representative images showing the rate of wound closure in the wound healing assay with shNC and shGPRC5A cell lines. 10× magnification: scale bar = 200 μm. (F,G) Representative fluorescence images (F) and macroscopic pictures (G) of liver metastases from CRLM models in the shNC and shGPRC5A groups (n = 6). (H–J) Liver weight (H), hematoxylin and eosin (H&E)-stained images (I), and liver metastatic burden (J) of mice injected with shNC or shGPRC5A cells (n = 6). 10× magnification: scale bar = 200 μm. $^{**}p < 0.01$, $^{***}p < 0.001$, $^{****}p < 0.0001$.

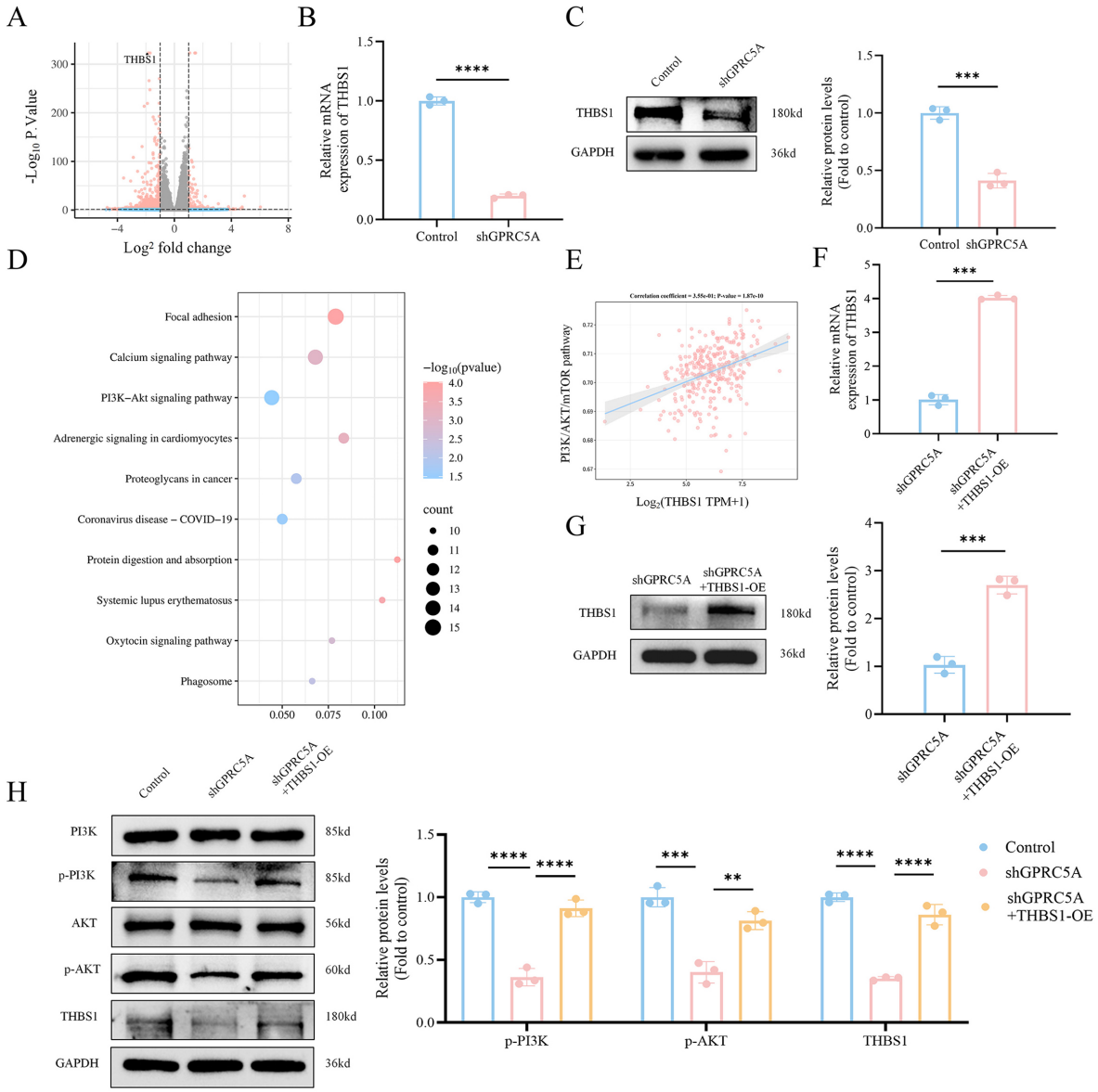


Fig. 3. GPRC5A is associated with thrombospondin 1 (THBS1) expression and phosphoinositide 3-kinase/protein kinase B (PI3K/AKT) phosphorylation. (A) Volcano plot showing upregulated and downregulated genes, with annotation of THBS1. (B,C) Expression of THBS1 at mRNA and protein levels in shNC and shGPRC5A cells (n = 3). (D) KEGG pathway enrichment analysis of the differentially expressed genes identified from RNA-seq data in shNC and shGPRC5A cell lines. (E) KEGG pathway association analysis. (F,G) THBS1 overexpression in CT26 cells was confirmed at mRNA and protein levels (n = 3). (H) Western blot assay confirming the activation status of the PI3K/AKT pathway (n = 3). $^{**}p < 0.01$, $^{***}p < 0.001$, $^{****}p < 0.0001$.

downstream effector of GPRC5A that drives the progression of liver metastasis through activation of PI3K/AKT phosphorylation. Our results provide novel insights into the molecular regulatory network that governs CRLM.

GPRC5A is a retinoic acid-inducible member of the GPCR superfamily that exhibits pronounced tissue-specific functional heterogeneity in cancer [7]. It is frequently silenced by promoter methylation and has tumor-suppressive properties in lung cancer, but functions as an oncogene in pancreatic cancer, breast cancer, and glioblastoma [16,17]. Previous bulk transcriptomic analyses in CRC have indicated that elevated GPRC5A expression in tumor tissue is correlated with lymph node metastasis and higher TNM stage. However, its expression profile and functional role specifically in liver metastasis have remained unexplored. The present study extends the oncogenic role of GPRC5A from primary CRC to liver metastases, demonstrating that it continues to drive metastatic outgrowth. Importantly, our results suggest that THBS1 may participate in the pro-metastatic effects associated with GPRC5A expression and PI3K/AKT signaling, although the precise mechanistic relationship requires further investigation.

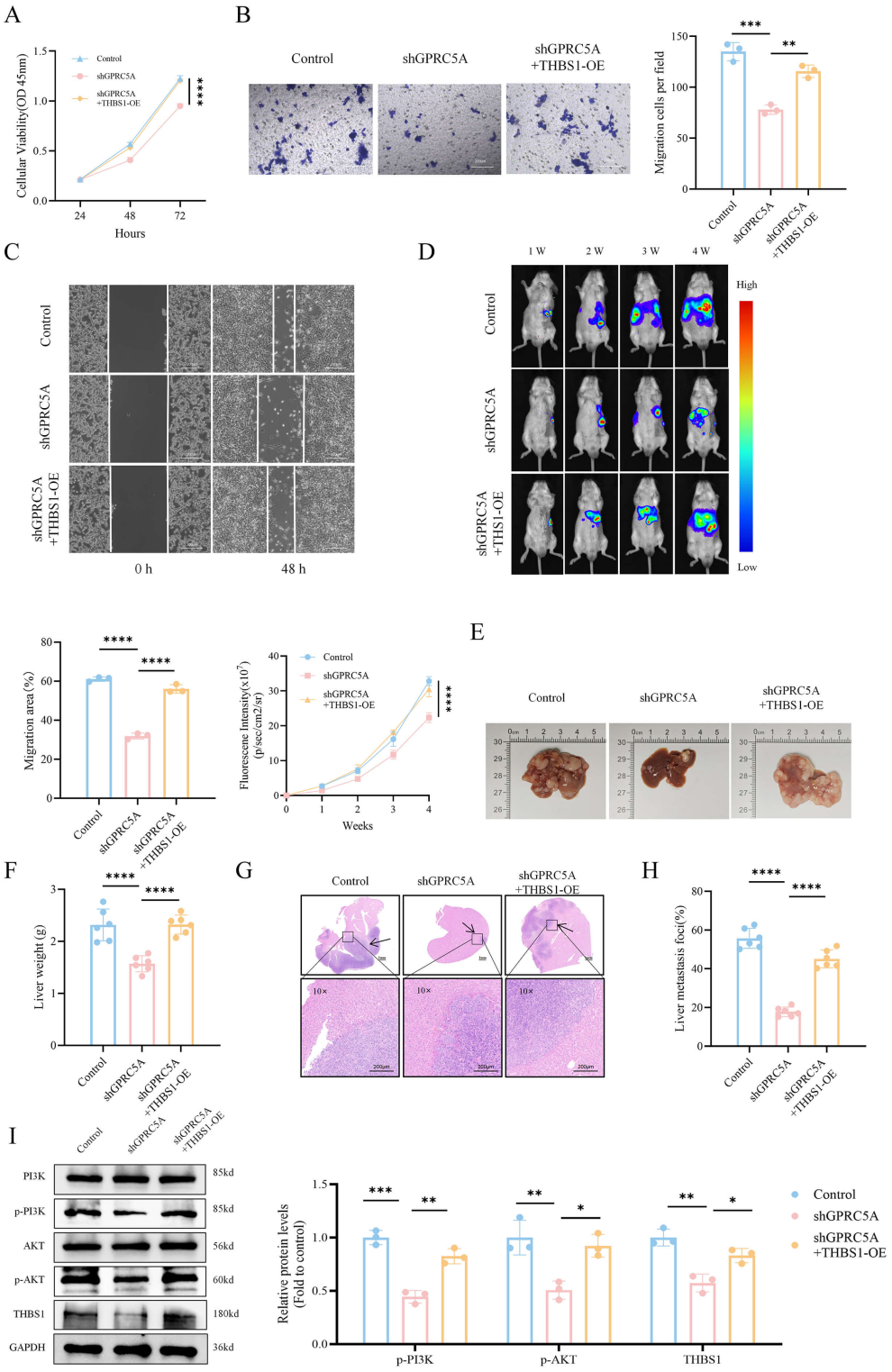


Fig. 4. GPRC5A promotes tumor progression in association with THBS1/PI3K/AKT signaling. (A) CCK-8 assay for the evaluation of cell viability (n = 6). (B) Representative images and number of cells from transwell assays in the Control, shGPRC5A, and shGPRC5A + THBS1-OE groups (n = 3). 10× magnification: scale bar = 200 μm. (C) Representative images showing the rate of wound closure in the wound healing assay in the Control, shGPRC5A, and shGPRC5A + THBS1-OE groups (n = 3). 10× magnification: scale bar = 200 μm. (D,E) Representative fluorescence images (D), and macroscopic images (E), of liver metastases from CRLM models in the Control, shGPRC5A, and shGPRC5A + THBS1-OE groups (n = 6). (F–H) Liver weight (F), H&E-stained images (G), and liver metastatic burden in the liver (H) of Control, shGPRC5A, and shGPRC5A + THBS1-OE mouse groups (n = 6). 10× magnification: scale bar = 200 μm. (I) Western blot assay verifies the PI3K pathway activation status in tissues (n = 3). *$p < 0.05$, **$p < 0.01$, ***$p < 0.001$, ****$p < 0.0001$.

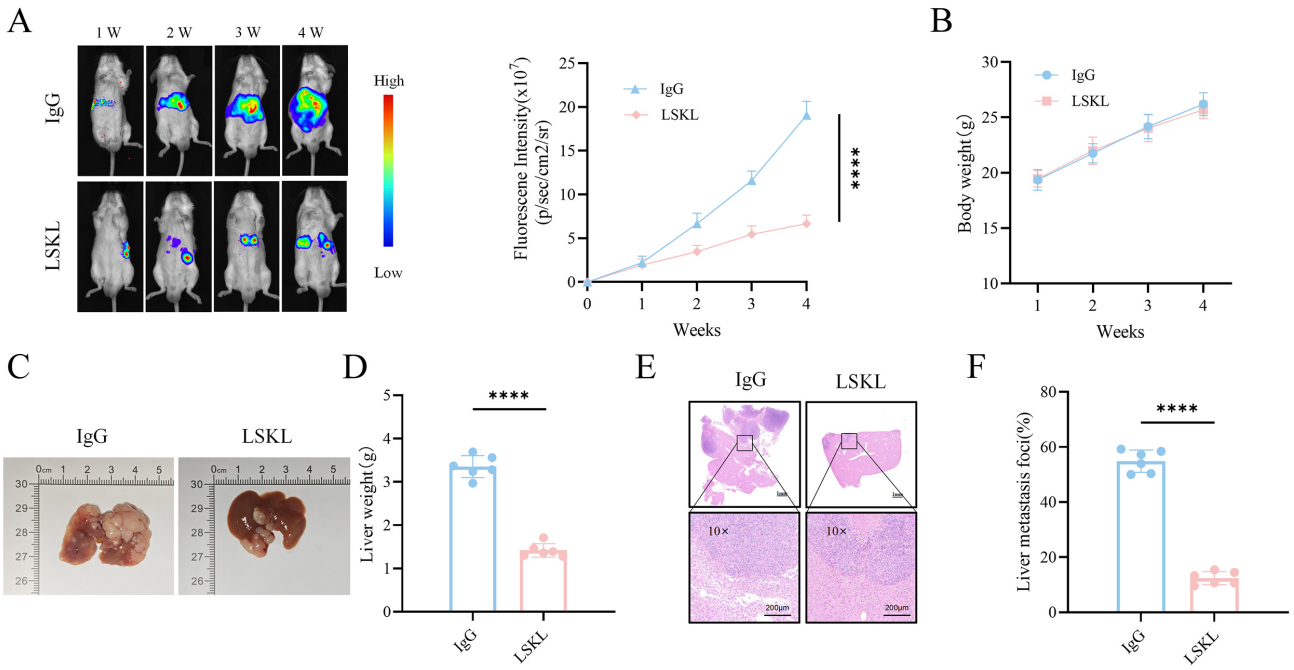


Fig. 5. Targeting THBS1 inhibits the progression of CRLM. (A) Representative fluorescence images of liver metastases from a murine CRLM model in the IgG (Control) and LSKL groups (n = 6). (B–F) Body weight (B), macroscopic images (C), liver weight (D), H&E-stained images (E), and burden of liver metastatic foci (F) in the Control and LSKL groups (n = 6). 10× magnification: scale bar = 200 μm. ****$p < 0.0001$.

THBS1 is a multidomain, secretory matricellular protein involved in tumor progression and metastasis. It was previously shown to exert dual functions in the tumor microenvironment (TME), including inhibition of angiogenesis and promotion of cell migration [18]. In several cancer types, high THBS1 expression is closely associated with an invasive phenotype and poor prognosis. For example, THBS1 can disrupt the integrity of endothelial cell junctions to promote local adhesion and tumor invasiveness in breast cancer [19,20]. It also facilitates cytoskeletal remodeling to promote cell dedifferentiation and pulmonary metastasis [21]. Despite these advances, the upstream regulatory mechanism of THBS1 in CRLM remains unknown. Our transcriptomic and molecular validation experiments demonstrated that GPRC5A knockdown significantly downregulated THBS1 mRNA and protein, and was accompanied by suppression of PI3K/AKT phosphorylation. Reconstitution of THBS1 partly restored the p-PI3K/p-AKT level, as well as the proliferation, migration, and liver metastatic capacity of tumor cells. Notably, changes in GPRC5A or THBS1 expression did not affect total PI3K and AKT protein levels but specifically modulated their phosphorylation status, indicating this axis functions by regulating signaling intensity rather than the abundance of pathway components. The substantial rescue of malignant phenotypes following THBS1 reconstitution suggests that THBS1 may contribute importantly to the pro-metastatic effects associated with GPRC5A, although the involvement of additional pathways cannot be excluded. This finding offers a mechanistic explanation for the sustained PI3K/AKT pathway activation observed in some liver metastases that lack canonical driver mutations, i.e., tumor cells maintain pro-metastatic signaling by upregulating the matricellular protein THBS1.

The PI3K/AKT signaling pathway is a key regulatory pathway governing tumor progression and metabolic adaptation [22,23]. It is frequently dysregulated in CRC and has been correlated with increased tumor cell proliferation, invasiveness, metastasis, and worse patient survival [24]. Mechanistically, activation of PI3K/AKT signaling promotes cell cycle progression, inhibits apoptosis, and facilitates the epithelial-mesenchymal transition, thereby enhancing the metastatic capacity of tumor cells [25]. Given its established involvement in oncogenic signaling, metabolic reprogramming, and tumor matrix interactions, the PI3K/AKT pathway may contribute to the development and progression of CRLM.

From a translational perspective, treatment with the THBS1 signaling blocker LSKL peptide significantly reduced liver metastatic burden in a mouse model without significant body weight loss. These findings suggest that targeting this signaling axis may have therapeutic potential and warrants further investigation. Given the involvement of THBS1 in angiogenesis, it would be interesting for future studies to explore whether combining LSKL with anti-angiogenic agents, such as bevacizumab, could provide ad-

ditional anti-metastatic benefits [26,27]. However, systemic inhibition of THBS1 could potentially affect wound healing and tissue homeostasis [28]. Liver-targeted delivery systems or TME-responsive nanocarriers may represent feasible strategies for more precise intervention [29,30].

5. Limitation

We acknowledge several limitations of this study. First, additional details of the transcriptional mechanism by which GPRC5A regulates THBS1 remain to be elucidated. Since GPRC5A lacks a typical DNA-binding domain, it may function as a coactivator in concert with other transcription factors to regulate THBS1 expression. Future studies employing ChIP-seq and promoter analyses are warranted. Second, the murine CRLM model was primarily based on intrasplenic injection of the CT26 cell line. However, the stromal and immune microenvironment of this model differs from that of human liver metastases. Future validation could involve humanized mouse models or patient-derived organoids [31]. The intrasplenic injection-induced CRLM model was primarily used to investigate the metastatic niche and TME within liver metastatic lesions. Third, the wound healing assay was conducted in the absence of cell proliferation inhibitors. Therefore, differences in proliferation rates may also contribute to the observed wound closure, representing a potential limitation of this assay. Fourth, because a THBS1 overexpression-alone group was not included, the extent to which THBS1 specifically mediates the effects of GPRC5A remains to be fully clarified. THBS1 may either function as a downstream effector of GPRC5A or exert independent pro-tumorigenic effects on cell proliferation, migration, and liver colonization. Furthermore, although GPRC5A showed predominantly cytoplasmic staining by IHC, this finding should be interpreted cautiously, as IHC alone does not directly establish its functional subcellular localization or biologically active pool. As an orphan GPCR, the endogenous ligand(s) and activation mechanisms of GPRC5A remain largely undefined. Although our data demonstrate that GPRC5A promotes THBS1 expression and metastatic progression, the precise signaling events connecting GPRC5A to THBS1 regulation require further mechanistic investigation. Finally, the value of GPRC5A and THBS1 as predictive biomarkers for liver metastasis should be evaluated in large prospective cohorts.

6. Conclusion

In conclusion, this study identified a THBS1-associated relationship between GPRC5A expression and PI3K/AKT pathway activation, which contributes to CRC liver metastasis. These results further elucidate the molecular regulatory network governing hepatic metastasis and provide an experimental foundation and theoretical rationale for metastasis-specific therapeutic strategies targeting the GPRC5A-THBS1 axis.

Availability of Data and Materials

The data generated in the present study may be requested from the corresponding author.

Author Contributions

LH and ZHD designed and performed the experiments, analyzed the data, and drafted the manuscript. MJL and XYJ conducted the experiments and acquired the data. WKY, CLL and WWL assisted with data analysis and interpretation. ChaZ and ChoZ conceived and supervised the study, secured funding, and critically revised the manuscript. All authors contributed to editorial changes in the manuscript. All authors read and approved the final manuscript. All authors have participated sufficiently in the work and agreed to be accountable for all aspects of the work.

Ethics Approval and Consent to Participate

The study was approved by the Ethics Committee of the First Affiliated Hospital of Anhui Medical University (Anhui, China) (approval number: Quick-PJ 2022-14-33). The study was carried out in accordance with the guidelines of the Declaration of Helsinki, and informed consent was provided by all patients. All mouse experiments were approved by the Animal Ethics Committee of Anhui Medical University (approval number: LLSC-20230579). The study was carried out in accordance with the ARRIVE guidelines. All animal experiments were conducted in accordance with the Guidelines for the Ethical Review of Laboratory Animal Welfare in China (GB/T 35892-2018) and the Guide for the Care and Use of Laboratory Animals (8th edition). The experimental procedures followed the principles of Replacement, Reduction, and Refinement (3Rs), with appropriate measures taken to minimize animal pain and distress.

Acknowledgment

Thanks to all the peer reviewers for their opinions and suggestions.

Funding

This work was supported by the University Research Project of Anhui Province (Grant nos 2025AHGXZK40773), the National Natural Science Foundation of China (Grant nos 82303475), the Inflammation and Immune Mediated Diseases Laboratory of Anhui Province (Grant nos IMMDL202406), the Quality Enhancement Project for New Era Education of Education Department of Anhui Province (Grant nos 2024zyxwjxalk048), the National Health Commission Capacity Building and Continuing Education Center (Grant nos GWJJMB202510022056).

Conflicts of Interest

The authors declare no conflicts of interest.

Supplementary Material

Supplementary material associated with this article can be found, in the online version, at https://doi.org/10.31083/FBL55797.

References

[1] Siegel RL, Giaquinto AN, Jemal A. Cancer statistics, 2024. CA: a Cancer Journal for Clinicians. 2024; 74: 12–49. https://doi.org/10.3322/caac.21820

[2] Bray F, Laversanne M, Sung H, Ferlay J, Siegel RL, Soerjomataram I, et al. Global cancer statistics 2022: GLOBOCAN estimates of incidence and mortality worldwide for 36 cancers in 185 countries. CA: a Cancer Journal for Clinicians. 2024; 74: 229–263. https://doi.org/10.3322/caac.21834

[3] Cervantes A, Adam R, Roselló S, Arnold D, Normanno N, Taïeb J, et al. Metastatic colorectal cancer: ESMO Clinical Practice Guideline for diagnosis, treatment and follow-up. Annals of Oncology. 2023; 34: 10–32. https://doi.org/10.1016/j.annonc.2022.10.003

[4] Shin AE, Giancotti FG, Rustgi AK. Metastatic colorectal cancer: mechanisms and emerging therapeutics. Trends in Pharmacological Sciences. 2023; 44: 222–236. https://doi.org/10.1016/j.tips.2023.01.003

[5] Li W, Yuan W, Du Z, Wang X, Wang D, Xing S, et al. AKR1B10 reprograms neutrophils by histone lactylation to foster immune evasion in KRASG12C mutation colorectal cancer liver metastasis. Journal of Experimental & Clinical Cancer Research. 2026; 45: 61. https://doi.org/10.1186/s13046-026-03653-2

[6] Tomás L, Raschzok N, Blanc E, Gallardo-Gómez M, Menne A, Astrahantseff K, et al. Cancer evolution and multi-omic profile of relapsed colorectal liver metastases after treatment. Genome Medicine. 2026; 18: 28. https://doi.org/10.1186/s13073-026-01614-0

[7] Iglesias González PA, Valdivieso ÁG, Santa-Coloma TA. The G protein-coupled receptor GPRC5A-a phorbol ester and retinoic acid-induced orphan receptor with roles in cancer, inflammation, and immunity. Biochemistry and Cell Biology. 2023; 101: 465–480. https://doi.org/10.1139/bcb-2022-0352

[8] Zhou H, Tan L, Zhang B, Kwong DLW, Wong CN, Zhang Y, et al. GPRC5A promotes lung colonization of esophageal squamous cell carcinoma. Nature Communications. 2024; 15: 9950. https://doi.org/10.1038/s41467-024-54251-9

[9] Zhou H, Telonis AG, Jing Y, Xia NL, Biederman L, Jimbo M, et al. GPRC5A is a potential oncogene in pancreatic ductal adenocarcinoma cells that is upregulated by gemcitabine with help from HuR. Cell Death & Disease. 2016; 7: e2294. https://doi.org/10.1038/cddis.2016.169

[10] Zhu T, Yang Q, Qian X, Wu X, Fang J, Lin Y, et al. GPRC5A/CXCL8/NLRP3-mediated neutrophil extracellular traps drive gemcitabine-nab-paclitaxel resistance in pancreatic adenocarcinoma. Cancer Biology & Medicine. 2025; 22: 832–853. https://doi.org/10.20892/j.issn.2095-3941.2025.0040

[11] Ou X, Tan Y, Xie J, Yuan J, Deng X, Shao R, et al. Methylation of GPRC5A promotes liver metastasis and docetaxel resistance through activating mTOR signaling pathway in triple negative breast cancer. Drug Resistance Updates. 2024; 73: 101063. https://doi.org/10.1016/j.drup.2024.101063

[12] Alafate W, Du S, Pan S, Lv G, Yang J, Cai H, et al. GPRC5A modulates resistance to temozolomide in glioblastoma through glycolytic reprogramming. International Journal of Biological Macromolecules. 2025; 321: 146390. https://doi.org/10.1016/j.ijbiomac.2025.146390

[13] Xu J, Zhang J, Li Y, Wang Z, Li Q, Liu A, et al. Tracing the stemness and malignant transition in a heritable colorectal cancer Lynch Syndrome by single-cell RNA-seq analysis. Frontiers in Immunology. 2026; 17: 1722806. https://doi.org/10.3389/fimmu.2026.1722806

[14] Chen Z, Li Y, He K, Yang J, Deng Q, Chen Y, et al. CircGPRC5A enhances colorectal cancer progress by stabilizing PPP1CA and inducing YAP dephosphorylation. Journal of Experimental & Clinical Cancer Research. 2023; 42: 334. https://doi.org/10.1186/s13046-023-02915-7

[15] Murphy-Ullrich JE, Suto MJ. Thrombospondin-1 regulation of latent TGF-β activation: A therapeutic target for fibrotic disease. Matrix Biology. 2018; 68–69: 28–43. https://doi.org/10.1016/j.matbio.2017.12.009

[16] Hu S, Chen Y, Sun B. Exploring the Prognostic Value and Immune Infiltration Patterns of GPRC5A Across Multiple Cancer Types. Journal of Cancer. 2024; 15: 4749–4758. https://doi.org/10.7150/jca.93217

[17] Jiang X, Xu X, Wu M, Guan Z, Su X, Chen S, et al. GPRC5A: An Emerging Biomarker in Human Cancer. BioMed Research International. 2018; 2018: 1823726. https://doi.org/10.1155/2018/1823726

[18] Kaur S, Bronson SM, Pal-Nath D, Miller TW, Soto-Pantoja DR, Roberts DD. Functions of Thrombospondin-1 in the Tumor Microenvironment. International Journal of Molecular Sciences. 2021; 22: 4570. https://doi.org/10.3390/ijms22094570

[19] Shen J, Cao B, Wang Y, Ma C, Zeng Z, Liu L, et al. Hippo component YAP promotes focal adhesion and tumour aggressiveness via transcriptionally activating THBS1/FAK signalling in breast cancer. Journal of Experimental & Clinical Cancer Research. 2018; 37: 175. https://doi.org/10.1186/s13046-018-0850-z

[20] Cen J, Feng L, Ke H, Bao L, Li LZ, Tanaka Y, et al. Exosomal Thrombospondin-1 Disrupts the Integrity of Endothelial Intercellular Junctions to Facilitate Breast Cancer Cell Metastasis. Cancers. 2019; 11: 1946. https://doi.org/10.3390/cancers11121946

[21] Xu E, Huang Z, Zhu K, Hu J, Ma X, Wang Y, et al. Thrombospondin 1 Promotes Cytoskeleton Remodeling, Dedifferentiation, and Pulmonary Metastasis through ITGA1 and ITGA6 in Osteosarcoma. International Journal of Biological Sciences. 2025; 21: 2083–2100. https://doi.org/10.7150/ijbs.93678

[22] Narayanankutty A. PI3K/ Akt/ mTOR Pathway as a Therapeutic Target for Colorectal Cancer: A Review of Preclinical and Clinical Evidence. Current Drug Targets. 2019; 20: 1217–1226. https://doi.org/10.2174/1389450120666190618123846

[23] Leiphrakpam PD, Batra R, Tenner L, Are C. Targeting Akt Signaling Pathway in Cancer: Molecular Mechanisms and Advances in Therapeutic Interventions. Frontiers in Bioscience (Landmark Edition). 2025; 30: 39100. https://doi.org/10.31083/FBL39100

[24] Minegishi K, Dobashi Y, Kimura E, Goto A. AKT: A Central Node in Complex Signaling Cascades. Frontiers in Bioscience (Landmark Edition). 2025; 30: 26414. https://doi.org/10.31083/FBL26414

[25] Maharati A, Moghbeli M. PI3K/AKT signaling pathway as a critical regulator of epithelial-mesenchymal transition in colorectal tumor cells. Cell Communication and Signaling: CCS. 2023; 21: 201. https://doi.org/10.1186/s12964-023-01225-x

[26] Zhao Y, Adjei AA. Targeting Angiogenesis in Cancer Therapy: Moving Beyond Vascular Endothelial Growth Factor. The Oncologist. 2015; 20: 660–673. https://doi.org/10.1634/theoncologist.2014-0465

[27] Lawler J. Thrombospondin-1 as an endogenous inhibitor of angiogenesis and tumor growth. Journal of Cellular and Molecular

Medicine. 2002; 6: 1–12. https://doi.org/10.1111/j.1582-4934.2002.tb00307.x

[28] Sweetwyne MT, Murphy-Ullrich JE. Thrombospondin1 in tissue repair and fibrosis: TGF-β-dependent and independent mechanisms. Matrix Biology. 2012; 31: 178–186. https://doi.org/10.1016/j.matbio.2012.01.006

[29] Tong F, Wang Y, Gao H. Progress and challenges in the translation of cancer nanomedicines. Current Opinion in Biotechnology. 2024; 85: 103045. https://doi.org/10.1016/j.copbio.2023.103045

[30] Vargason AM, Anselmo AC, Mitragotri S. The evolution of commercial drug delivery technologies. Nature Biomedical Engineering. 2021; 5: 951–967. https://doi.org/10.1038/s41551-021-00698-w

[31] Zhou B, Feng Z, Xu J, Xie J. Organoids: approaches and utility in cancer research. Chinese Medical Journal. 2023; 136: 1783–1793. https://doi.org/10.1097/CM9.0000000000002477